Article

Engineering Achiral Liquid Crystalline Polymers for Chiral Self-Recovery

Tengfei Miao, Xiaoxiao Cheng, Yilin Qian, Yaling Zhuang and Wei Zhang *

State and Local Joint Engineering Laboratory for Novel Functional Polymeric Materials, Jiangsu Engineering Laboratory of Novel Functional Polymeric Materials, College of Chemistry, Chemical Engineering and Materials Science, Soochow University, Suzhou 215123, China; mtf0824@163.com (T.M.); studentscheng@163.com (X.C.); ylqian@stu.pku.edu.cn (Y.Q.); sa21175113@mail.ustc.edu.cn (Y.Z.)
* Correspondence: weizhang@suda.edu.cn; Tel.: +86-512-6588-4243

Abstract: Flexible construction of permanently stored supramolecular chirality with stimulus-responsiveness remains a big challenge. Herein, we describe an efficient method to realize the transfer and storage of chirality in intrinsically achiral films of a side-chain polymeric liquid crystal system by combining chiral doping and cross-linking strategy. Even the helical structure was destroyed by UV light irradiation, the memorized chiral information in the covalent network enabled complete self-recovery of the original chiral superstructure. These results allowed the building of a novel chiroptical switch without any additional chiral source in multiple types of liquid crystal polymers, which may be one of the competitive candidates for use in stimulus-responsive chiro-optical devices.

Keywords: chiral induction; chiral self-recovery; supramolecular chirality; chiral nematic phase

1. Introduction

Chirality, a fundamental property of nature, usually plays an essential role in biological processes and living systems. Nature is expert in using simple building blocks to efficiently fabricate highly complex systems, as well as the elegant assembly that can exhibit a variety of excellent performance [1,2]. Inspired by this, research on the transfer, amplification and memory of chirality between multi-levels, including secondary, tertiary and quaternary structures, is of key importance for understanding the origin of homochirality, as well as for the possible development of novel chiral materials [3–5].

Manipulating and memorizing hierarchically assembled chiral structures in achiral matters is an everlasting curiosity for scientists due to the avoidance of expensive chiral raw materials or tedious synthesis [6–10]. Meanwhile, chirality transfer from the chiral additive to achiral polymer chains via non-covalent interactions is a vital respect for propelling their applications in chiral sensors, chiroptical switches, chiral recognition and asymmetric catalysis [11]. Up-to-date, chiral solvation [12–14], circularly polarized light (CPL) [15–17], chiral liquid crystal field [18,19] and chiral template/scaffold [20–22] are candidates to generate macromolecular or supramolecular chirality in achiral polymer systems. However, the chiral supramolecular structures formed by non-covalent interactions between achiral building blocks are often easily destroyed by external stimulus [23–25], which undoubtedly limits the application of chiral materials. Typically, the chirality cannot be restored in the absence of pre-chiral resources. It can be speculated that constructing permanently memorized chirality with superior controllability or self-recovery capability in an achiral polymer system remains an extreme challenge. To achieve this, the adoption of covalent fixation after self-assembly via cross-linking of polymer chains will be a good choice [26].

The fascinating helical superstructure in the liquid crystal (LC) state is a striking example that reveals the structure–property relationship [27,28]. Similarly, introducing mirror symmetry breaking into LCs will commonly result in multitudinous chiral LC phases, such as the chiral nematic (N*) [29,30], chiral smectic (S*) [31], twist grain boundary (TGB) [32]

and cubic blue phases [33], which have been well investigated in small molecular LCs. As reported by Li et al. [34–36], the sign and the magnitude of the N*-LCs pitches are strongly governed by chiral dopants due to their good fluidity. From another point of view, good fluidity is often accompanied by poor stability and a strong dependence on chiral resources. Among the self-organized supramolecular systems, chiral liquid crystalline polymers (LCPs) represent a promising class of materials that might exhibit stable supramolecular helical organizations [37,38]. Usually, the induced chirality can only be temporarily stored in the achiral systems through the interactions between polymer chains but will be completely destroyed when undergoing a phase transition [39]. Combining the cross-linking strategy and self-organization of achiral mesogens in side-chain liquid crystalline polymers, we set out to develop a novel, controllable helical structure where the induced chiral information can be stored permanently and be able to spontaneously trigger the self-recovery of original chiral superstructures even after being completely destroyed.

We have previously reported the induction and storage of supramolecular chirality via chiral limonene vapor fumigation and cross-linking in achiral polymer chains containing π-π conjugated azobenzene groups [40]. However, whether the supramolecular chirality can be induced and stored in the muti-types of liquid crystalline polymers such as the polymer containing non-coplanar mesogens cyanobiphenyl (CNB) or the phenyl benzoate (PB) group remains to be explored. Moreover, dynamically controlling the chiral signal intensity and the "on-off" chiroptical switch in the above polymer systems has rarely been achieved.

2. Results and Discussion

In the current work, a series of liquid crystalline polymers were synthesized with controlled molecular weights (M_ns) and molecular weight distributions via reversible addition-fragmentation chain transfer (RAFT) polymerization. The non-coplanar mesogens, cyanobiphenyl (CNB) or phenyl benzoate (PB) groups were introduced into the polymer as side chains for chiral self-organization. Besides, the hydroxyl-azobenzene, the photosensitive cross-linkable LC group [41,42], was also adopted to allow the regulation and permanent memory of the induced helical superstructure. The structures of the achiral polymers (PCNBMA$_{1-5}$, PPBMA$_{1-5}$ and PPBMA-r-AzOH) and chiral dopants are listed in Figure 1. The synthetic routes to the monomers (CNBMA, PBMA and AzOH) and polymers have been described in Scheme S1. As shown in Table 1 and Figures S1–S3, the polymers with different M_ns were successfully prepared by changing the relative molar ratios of monomers and chain transfer agent (CTA). The small chiral molecules (PB-R/S1, PB-R/S5, CNB-R/S1 and CNB-R/S5) were successfully synthesized and determined by ^{1}H NMR spectra and chiral high-performance liquid chromatography (HPLC) (Figures S4–S6).

Table 1. Molecular weight characteristics of liquid crystalline polymers.

Entry	Ratio [1]	Conv. [2] (%)	$M_{n(GPC)}$ [3] (g/mol)	M_w/M_n [3]
PPBMA$_1$	40:3:1	59.7	3500	1.17
PPBMA$_2$	100:3:1	50.2	7300	1.12
PPBMA$_3$	200:3:1	41.6	8200	1.23
PPBMA$_4$	300:3:1	32.9	11,100	1.21
PPBMA$_5$	500:3:1	22.7	15,200	1.17
PPB-*r*-AzOH	60:40:3:1	46.6	8800	1.14
PCNBMA$_1$	40:3:1	61.6	3300	1.12
PCNBMA$_2$	100:3:1	56.3	7600	1.18
PCNBMA$_3$	200:3:1	40.9	10,700	1.14
PCNBMA$_4$	300:3:1	29.3	12,300	1.20
PCNBMA$_5$	500:3:1	21.3	15,600	1.21

[1] Polymerization conditions for PPBMA$_{1-5}$ and PCNBMA$_{1-5}$: [monomer]$_0$/[CPDN]$_0$/[AIBN]$_0$. Polymerization conditions for PPB-*r*-AzOH: [PBMA]$_0$/[AzOH]$_0$/[CPDN]$_0$/[AIBN]$_0$). [2] Determined gravimetrically. [3] Determined by GPC according to PS standards in THF.
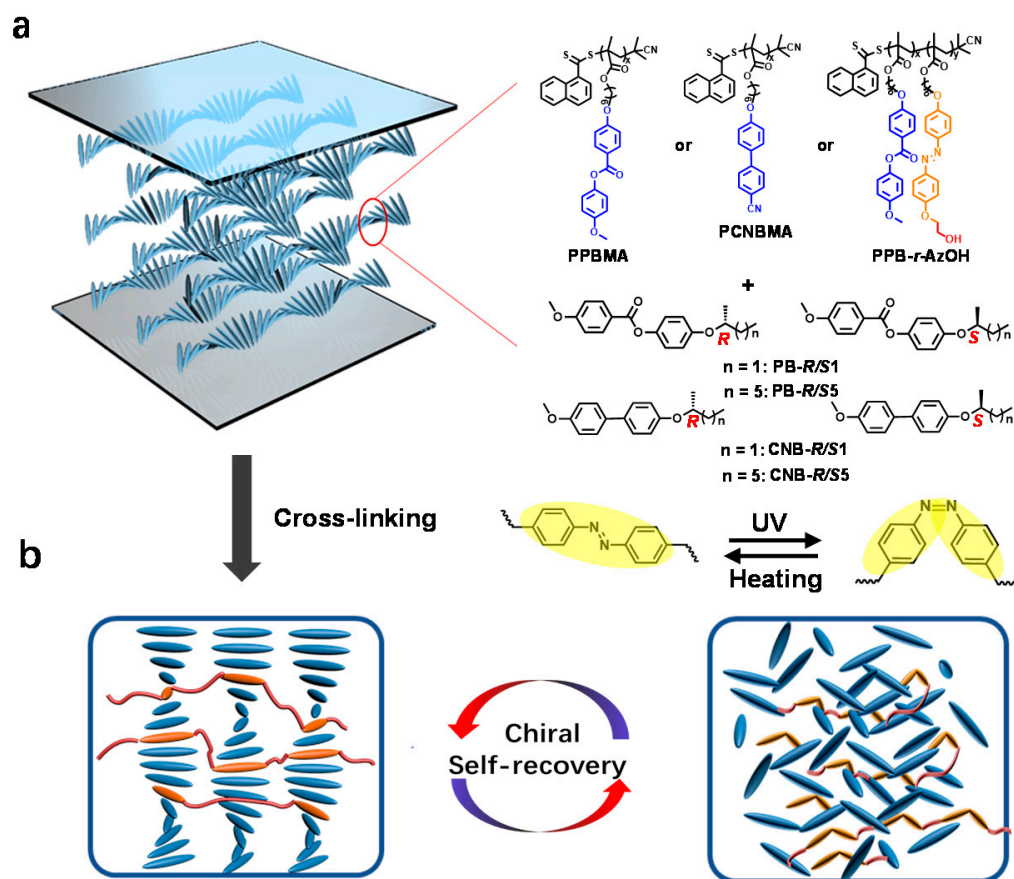
Figure 1. (**a**) Schematic representation of the chiral nematic phase formed from the achiral polymers and chiral dopants. (**b**) Process of the locking and self-recovery of the induced chirality.

First of all, the formation of the chiral nematic phase was investigated and determined using differential scanning calorimetry (DSC), small-angle X-ray scattering instrument (SAXS) and polarized optical microscope (POM) (Figures S7–S9). After being doped with a certain amount of chiral dopant, no scattering peak was observed both in the mixture of PPBMA/PCNBMA and PB-R1/CNB-R1 (Figure S8), indicating the absence of any layer structure corresponding to the smectic phase. Besides, the typical fingerprint textures of the chiral nematic phase were clearly observed when undergoing an appropriate annealing process (Figure S9). It can be speculated that the orientation of the mesogens in polymer side chains (PBs or CNBs) are slightly twisted with respect to their neighbors under the command of chiral dopants, leading to a long-range helical periodic superstructure [43].

Chirality transfer from the chiral dopant to achiral polymers in solid-state film (prepared from THF solution containing achiral polymers and chiral dopants, as described in experimental methods) was then explored in detail by UV-vis and circular dichroism (CD) spectroscopy (Figure 2). The strong absorption bands from 230 nm to 300 nm and from 250 nm to 350 nm are attributed to the π-π* transition of the cyanobiphenyl and phenyl benzoate group, respectively. Originally, both the PPBMA and PCNBMA films exhibited a weak Cotton effect in the CD spectra when doped with chiral molecules. As expected, intense CD signals consisting of two overlapped exciton couplets that correspond to the π-π* transitions of PBs or CNBs units were clearly detected when increasing the temperature (Figure 2). A positive sign at the first Cotton band and a negative sign at the second Cotton band were observed when the PB/CNB-R1 was employed. Conversely, PB/CNB-S1 exhibited a mirror-image Cotton effect. It should be noted that the optically active polymer films show completely opposite Cotton effect when doped with PB/CNB-R5 or PB/CNB-S5 as compared with PB/CNB-R1 or PB/CNB-S1. We can speculate that the

helical direction can be controlled not only by the configuration but also by the alkyl chain length of the chiral dopants.
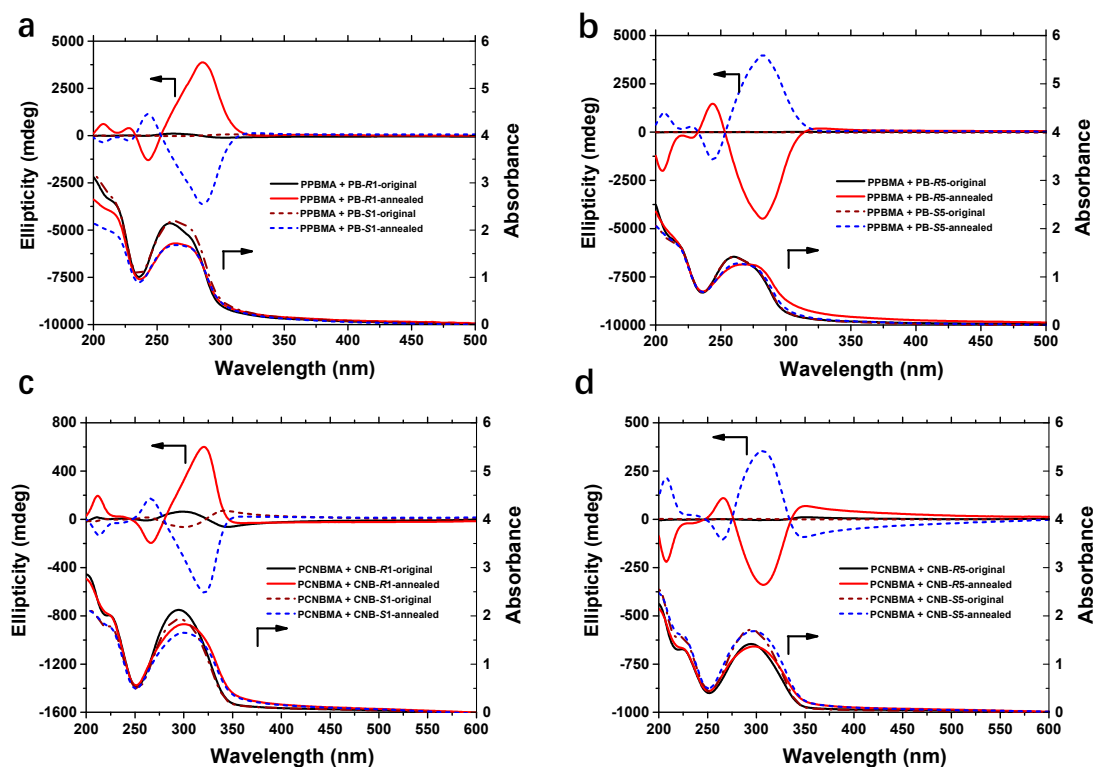

Figure 2. Chiral expression of the polymer films containing different components. (**a**) CD and UV-vis spectra of PPBMA$_3$ doped with PB-*R/S*1. (**b**) CD and UV-vis spectra of PPBMA$_3$ doped with PB-*R/S*5. (**c**) CD and UV-vis spectra of PCNBMA$_3$ doped with CNB-*R/S*1. (**d**) CD and UV-vis spectra of PCNBMA$_3$ doped with CNB-*R/S*5.

Besides, the enhancement of CD signals indicates that the non-polar mesogens in the polymer side chains self-organized into a preferential chiral structure via cooperative interactions with the chiral dopants. The observed CDs are not the contribution of dopants in polymer film but mainly derived from the helical structure of polymers because no obvious CD decline can be found when chiral polymer films were immersed in methanol to remove the chiral dopants, as described in Section 3.3 and Figure S10. Temperature plays an important role during the chiral induction process due to the instability of the chiral nematic phase. The evolution of the CD spectra of polymer films during the heating process was tracked in detail. As shown in Figure 3a–d, CD intensity increased with increasing temperature until reaching their maximum values at around 72 °C (PPBMA films) and 80 °C (PCNBMA films). More prolonged heating of the polymer films resulted in a deep decrease in CD intensity ascribed to the fluidity of the nematic phase. Increasing the relative molar ratio of the dopant caused an enhancement in the intensity of ellipticity values (Figure 3e,f), which may be ascribed to the decrease in helical pitch ($\beta = (pc)^{-1}$, β: helical twisting power of the dopant, p: helical pitch, c: the content of the dopant). The decrease in helical pitch means the increase of dihedral angles of two exciton couplets (much smaller than the extreme case, according to Nina's exciton theory) [44].

The polymer films containing PPBMA$_{1-5}$ and PCNBMA$_{1-5}$ with different M$_n$s were prepared to investigate the effect of the polymer molecular weights on chiral induction. After chiral doping and heating–cooling treatment, the maximum g$_{CD}$ values for each polymer film were recorded. As presented in Figure 4, the absolute maximum g$_{CD}$ values of PPBMAs or PCNBMAs first increased and then decreased with the molecular weight after reaching their maximum values (PPBMA$_3$, 8200 g/moL and PPBMA$_4$, 12,300 g/moL), respectively.
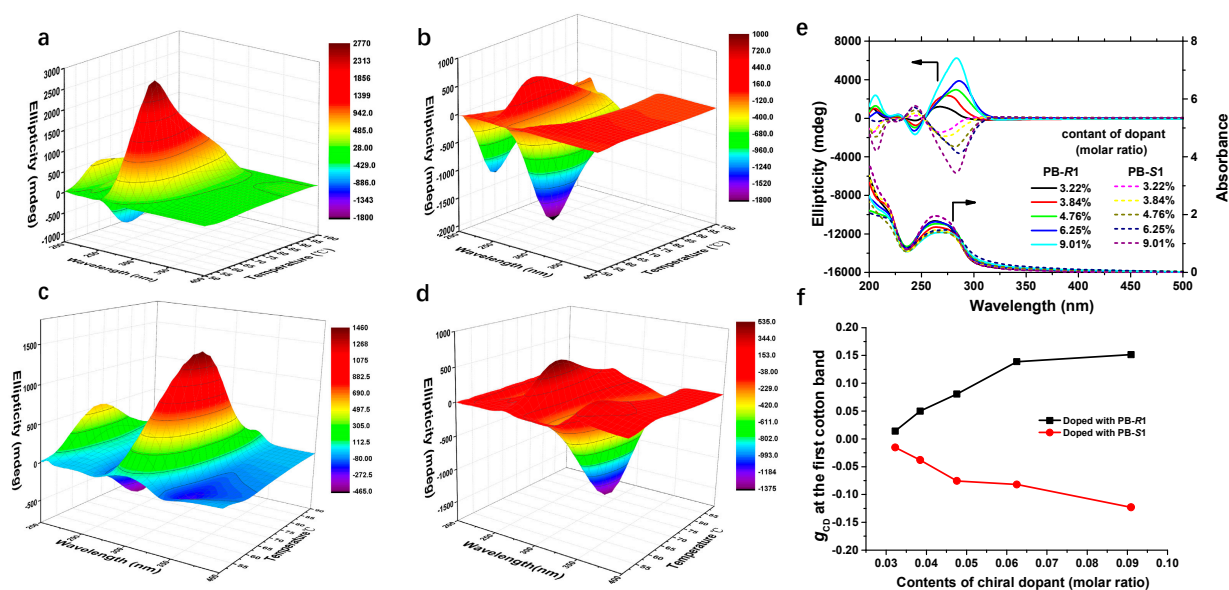
Figure 3. (**a**–**d**) CD spectra of the chiral induction of different polymer films during the heating process. (**a**) PPBMA$_3$ film doped with PB-*R*1. (**b**) PPBMA$_3$ film doped with PB-*S*1. (**c**) PCNBMA$_3$ doped with CNB-*R*1. (**d**) PCNBMA$_3$ doped with CNB-*S*1. (**e**) CD and UV-vis spectra of PPBMA$_3$ doped with different content of PB-*R*1 and PB-*S*1. (**f**) g_{CD} values of PPBMA$_3$ doped with different content of PB-*R*1 and PB-*S*1, calculated from (**e**).
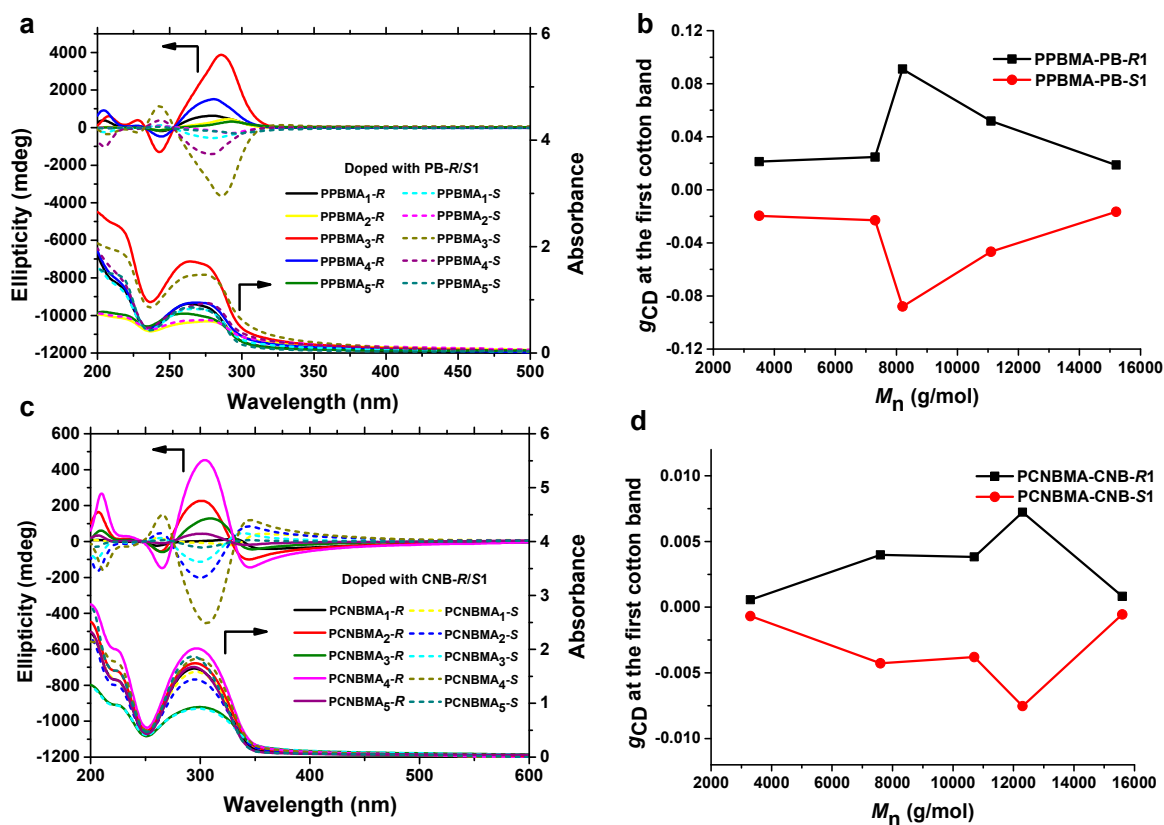
Figure 4. Changes in CD, UV-vis spectra and g_{CD} values of polymer films prepared from the polymers with different molecular weights. (**a**,**b**) recorded from PPBMAs. (**c**,**d**) recorded from PCNBMAs.

In order to flexibly control and permanently store the induced supramolecular chirality in the achiral polymer systems, photoisomerizable azobenzene units containing hydroxyl at a terminal for covalent cross-linking were introduced into the polymer side chain. Firstly,

the chiral order of PPB-r-AzOH induced by chiral dopant was studied by CD spectra. After heating the polymer film (doped with PB-R1) to 90 °C, a positive sign of the first Cotton band at 400 nm appeared, which is due to the π-π* transitions of chirally arranged E-azobenzene units. However, no exciton couplet center was seen in the CD spectrum, and the second positive and weaker Cotton band at around 280 nm was found (Figure 5a). This is caused by the overlapping between the second weaker Cotton band belonging to azobenzene (negative) and the first stronger Cotton band belonging to phenyl benzoate (positive). Mirror-image Cotton effects were observed in the case of doping with PB-S1. Then the polymer film was immersed in methanol to remove the chiral dopant (see Section 3.3). The removal of chiral dopant from polymer film was confirmed by ^{1}H NMR and HPLC spectra. As shown in Figure S11, the complete disappearance of the dopant signal indicates that the small chiral molecules have been removed successfully. The immersing process had no obvious effect on the CD spectra (Figure S14a). After chiral induction and the removal of the chiral source, the copolymer films were placed into an HCHO and HCl vapor atmosphere for covalent cross-linking via acetal reaction (Figure 5b). Differences in solubility of polymer films before and after cross-linking in THF revealed the success of cross-linking reactions (Figure 5d). Importantly, the chiral structure was perfectly preserved throughout the cross-linking procedure, as confirmed by the almost identical ellipticity values in CD spectra (Figure 5c).
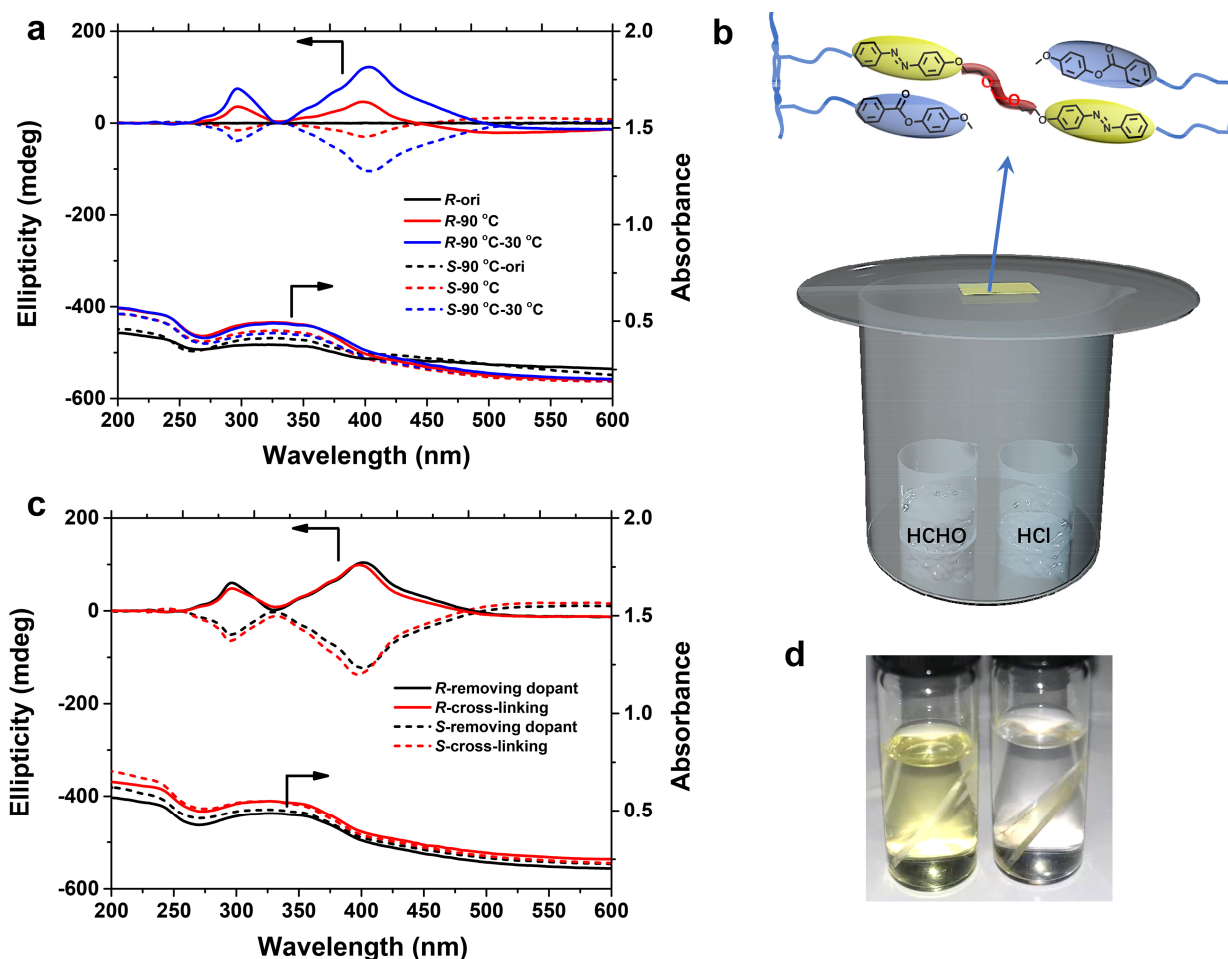
Figure 5. (**a**) CD and UV-vis spectra of the copolymer (PPB-*r*-AzOH) films doped with PB-*R*/*S*1. (**b**) Schematic diagram of the reaction method during the cross-linking process. (**c**) CD and UV-vis spectra of the chiral films after removing chiral dopants and after cross-linking reaction. (**d**) Pictures of the chiral polymer films placed in THF solution (left, before cross-linking; right: after cross-linking).

Distinct from uncross-linked counterparts, the cross-linked PPBMA films exhibited superior thermal stability even in the absence of chiral dopant. When heating the film to a high temperature (105 °C), a slight decrease of CD intensity occurred ascribed to partial fluidity of mesogenic units. The shape of the CD spectra remained almost unchanged with extended heating time and recovered to the original state after cooling down the films to room temperature (Figure S12). We further investigated the chiral self-recovery behavior of the supramolecular structure upon exposure to UV light irradiation. As reported previously, the trans forms of some Azo derivatives exhibited a nematic phase, whereas their cis forms showed no LC property [45]. For chiral PPB-r-AzOH films, UV-vis spectra showed a clear decline at 365 nm (π-π* electronic transition of the trans isomers) and an increase at 450 nm (n-π* electronic transition of the cis isomers) upon irradiation with 365 nm light, demonstrating the trans−cis photoisomerization of the Azo groups (Figure 6a). After 1500 s of irradiation, the regular helical structures of both the phenyl benzoate and azobenzene portion were completely disrupted, as confirmed by the disappearance of the CD signals (Figure 6b). Traditionally, the presence of a chiral source is necessary both in solution or solid films for the "on-off" chiroptical switch [46,47]. Interestingly, as displayed in Figure 6c, the shapes and intensities of CD spectra can return to their original states by a simple heating–cooling treatment (heated to 95 °C, maintained for 3 min before cooling down to room temperature). The uncross-linked chiral polymer films will lose the chiral information when they are irradiated by UV light after removing the dopants s (Figure S14). It can be speculated that the cross-linked organized Azo units can provide cryptochirality to trigger the complete self-recovery of the entire chiral superstructure. This means that the chiral information from an external source can be permanently memorized in achiral polymer systems.
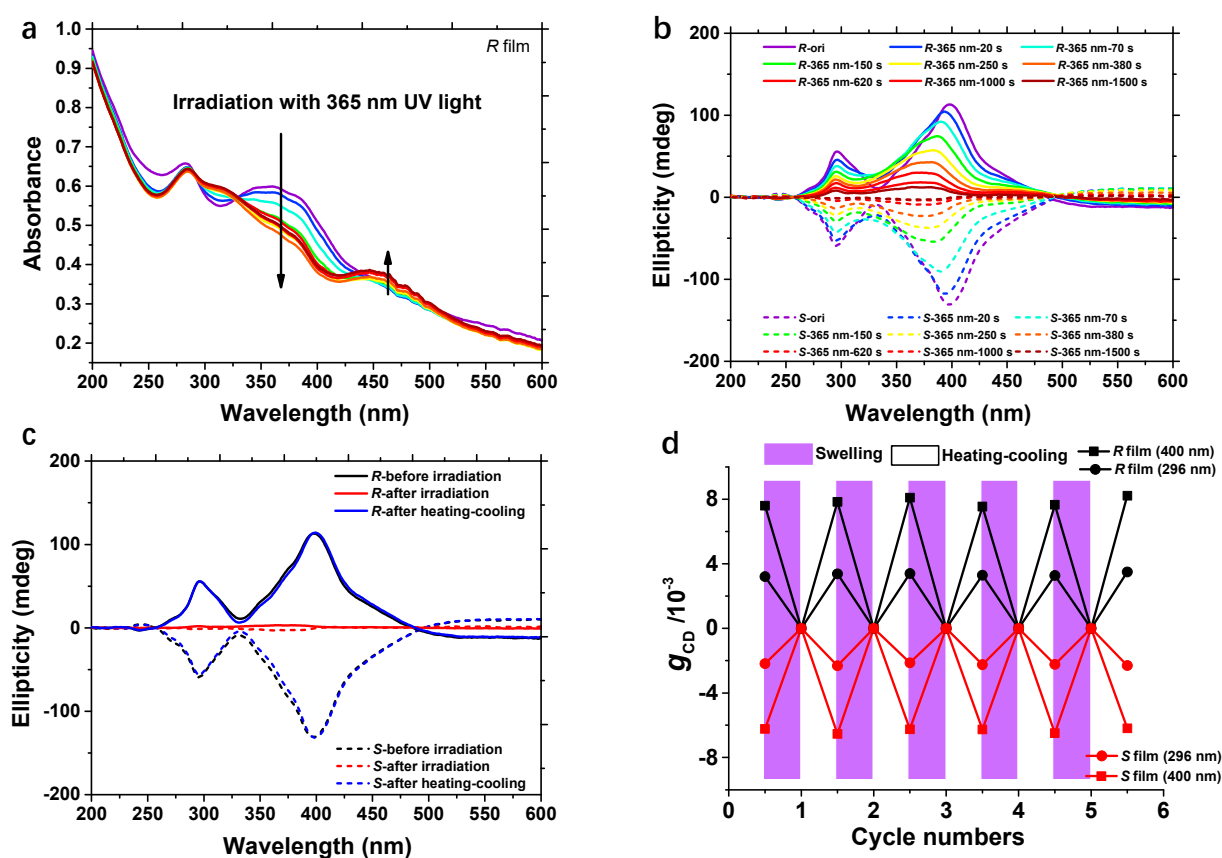
Figure 6. (**a**) Changes in UV-vis spectra of the cross-linked chiral polymer films under irradiation with 365 nm light. (**b**) Changes in CD spectra of the cross-linked chiral polymer films (induced by PB-*R*/*S*1) during 365 nm light irradiation. (**c**) Self-recovery of CD signals of the irradiated chiral films during the heating–cooling process. (**d**) Construction of chiroptical switch without chiral resource: destruction and chiral self-recovery behavior: switches of the cross-linked films during the above process (as shown by g_{CD} values, calculated from Figure S15).

The reversible chiral–achiral switching can enhance the functionality of optically active materials. Indeed, the traditional approach always involves sophisticated design and noticeable dependence on the chiral source. Combining the chiral doping and cross-linking strategy, a chiroptical switch based on the absolute achiral polymer can be successfully constructed. The above "on-off" switching could be repeated at least five times without any noticeable loss in CD intensity (Figures 6d and S15).

3. Materials and Methods

3.1. Materials

Chiral alcohols including (R)-(-)-butanol (>99.0%, TCI), (S)-(+)-butanol (>98.0%, TCI), (R)-(-)-octanol (>99%, TCI) and (S)-(+)-octanol (>99%, TCI) were used without further purification. Moreover, 6-Chlorohexyl methacrylate, 4-(2-hydroxy ethoxy)-4'-(2-hexyloxy methacrylate) azobenzene (AzOH) were synthesized as reported previously [40]. The compounds 4-methoxyphenyl 4-hydroxybenzoate, 4-cyano-4 -hydroxybiphenyl and 4-hydroxy-4-methoxybiphenyl were purchased from Sigma-Aldrich (St. Louis, MO, USA). The preparation steps for achiral monomers PBMA, CNBMA, chiral dopants and liquid crystalline polymers were listed in supplementary materials.

3.2. Preparation of the Chiral Polymer Films

The achiral polymer films for CD measurements with thickness ranging from 100 to 200 nm were prepared by spin coating the polymer solution (12 mg/mL in THF, doped with a certain number of chiral molecules) onto a clean quartz plate at a speed of 0.5 rpm for 6 s and following a speed of 1.9 rpm for 20 s. After drying under vacuum to remove THF, the film was heated to the nematic temperature to ensure the occurrence of chiral transmission.

3.3. Removal of Chiral Dopants

The chiral polymer film containing chiral dopants was immersed in methanol for 50 h to remove the chiral dopants, during which the immersing liquid was changed at least six times. After that, the residual amount of chiral dopant in polymer films was measured by ^{1}H NMR and HPLC spectroscopy (Figure S11).

3.4. The Storage of the Supramolecular Chirality

After chiral induction and removal of the dopants, the chiral copolymer PPB-r-AzOH films were placed on the top of a larger beaker in which two small beakers containing 30% formaldehyde aqueous and 6 N hydrochloric acid solution were placed separately (Figure 5b). Then the cross-linking of the polymer chains was carried out during the exposure to HCl and HCHO vapor at 25 °C for 20 h. Finally, the cross-linked polymer films were washed with pure water to remove the residual HCl and HCHO molecules and then dried under vacuum at 35 °C for 12 h.

3.5. Photoisomerization Process of Polymer Films

Photoisomerization of cross-linked chiral copolymer film was conducted with a 500 W high-pressure mercury lamp (Tokyo, Japan), Optiplex SX-UID and 502HUV) equipped with a narrow bandpass filter for the wavelength of 365 nm. The intensity of UV light irradiation is 2.5 mW cm^{-2}.

3.6. Characterization

^{1}H NMR spectra were recorded on a Bruker nuclear magnetic resonance instrument (300 MHz, Brucker, Karlsruhe, Germany) using CDCl$_3$ and DMSO-d$_6$ as solvent and tetramethylsilane (TMS) as the internal standard at room temperature.

Gel-permeation chromatography (GPC) measurements were conducted on the TOSOH HLC-8320 gel permeation chromatography (GPC) (TOSOH, Japan), equipped with refractive index and UV detectors using two TSKgel SuperMultiporeHZ-N (4.6 × 150 mm, 3.0 μm

beads size) columns arranged in series. Polymers can be separated in the molecular weight range of 500–190k Da. THF was used as the eluent with a flow rate of 0.35 mL/min at 40 °C. The number average molecular weights (M_n) and molecular weight distributions (M_W/M_n) of samples were calculated according to polystyrene (PS) standards.

The phase transition of the polymers was measured with a TA-Q100 DSC instrument (TA, New Castle, DE, USA). The temperature range is 20 °C to 200 °C with the first heating–cooling speed of 20 °C/min and second heating speed of 10 °C/min.

LC textures and birefringence of the samples were examined under a POM (Olympus Corporation, BX51-P, Japan) equipped with a hot stage (Linkam THMS600).

SAXS experiments were performed with a high-flux X-ray instrument (SAXSess mc^2, Anton Paar, Austria) equipped with a line collimation system and a 2200 W sealed-tube X-ray generator (CuKα, λ = 0.154 nm). The polymer samples were wrapped in aluminum foils and sandwiched in a steel sample holder.

The CD spectra were recorded on a JASCO J-1500 spectropolarimeter equipped with a Peltier-controlled housing unit using an SQ-grade cuvette, a single accumulation, a bandwidth of 2 nm, a scanning rate of 200 nm/min, a path length of 10 mm and a response time of 1 s. The magnitude of the circular polarization at the ground state is defined as $g_{CD} = 2 \times (\varepsilon_L - \varepsilon_R)/(\varepsilon_L + \varepsilon_R)$, where ε_L and ε_R denote the extinction coefficients for left and right circularly polarized light, respectively. Experimentally, g_{CD} value is defined as $\Delta\varepsilon/\varepsilon$ = [ellipticity/32,980]/absorbance at the CD extremum. The UV-vis spectra were recorded on a UV-2600 spectrophotometer (Shimadzu (Nakagyo-ku, Kyoto, Japan)).

Chiral HPLC was performed on an Agilent 1200 Series chromatography (Agilent, California USA) using a Daicel Chiralpak AD-H column (0.46 cm × 25 cm).

4. Conclusions

In summary, we have demonstrated a novel approach to construct an optically active polymer film with adjustable and permanently memorized supramolecular chirality via chiral doping and cross-linking. Side-chain liquid crystalline polymers containing non-coplanar mesogens CNB or PB were adopted as achiral hosts. We have investigated the influence of temperature, molecular weight, dopant structure and contents on the chiral expression in detail. Furthermore, introducing cross-linkable azobenzene units allows the photo regulation and storage of the induced chirality, which enables the construction of a chiroptical switch in the absence of chiral sources. Our research will pave a novel and efficient way for the design and construction of functional chiral polymer materials with reversible chiroptical properties from absolute achiral building blocks.

Supplementary Materials: The following are available online at https://www.mdpi.com/article/10.3390/ijms222111980/s1.

Author Contributions: T.M., X.C., Y.Q. and Y.Z. performed the experiments. T.M. organized the data and wrote the manuscript. W.Z. designed the experimental plan and revised the manuscript. All authors have read and agreed to the published version of the manuscript.

Institutional Review Board Statement: Not applicable.

Informed Consent Statement: Not applicable.

Data Availability Statement: No datasets have been used for this study.

Conflicts of Interest: The authors declare no conflict of interest.

References

1. Vignolini, S.; Rudall, P.J.; Rowland, A.V.; Reed, A.; Moyroud, E.; Faden, R.B.; Baumberg, J.J.; Glover, B.J.; Steiner, U. Pointillist structural color in pollia fruit. *Proc. Natl. Acad. Sci. USA* **2012**, *109*, 15712–15715. [CrossRef] [PubMed]
2. Aldersey-Williams, H. Towards biomimetic architecture. *Nat. Mater.* **2004**, *3*, 277–279. [CrossRef] [PubMed]
3. Yin, L.; Miao, T.-F.; Cheng, X.-X.; Jiang, Z.-C.; Tong, X.; Zhang, W.; Zhao, Y. Chiral liquid crystalline elastomer for twisting motion without preset alignment of mesogens. *ACS Macro Lett.* **2021**, *10*, 690–696. [CrossRef]
4. Cheng, X.X.; Miao, T.F.; Yin, L.; Ji, Y.J.; Li, Y.Y.; Zhang, Z.B.; Zhang, W.; Zhu, X.L. In situ controlled construction of a hierarchical supramolecular chiral liquid-crystalline polymer assembly. *Angew. Chem. Int. Ed.* **2020**, *59*, 9669–9677. [CrossRef]
5. Huang, S.; Chen, Y.X.; Ma, S.D.; Yu, H.F. Hierarchical self-assembly in liquid-crystalline block copolymers enabled by chirality transfer. *Angew. Chem. Int. Ed.* **2018**, *57*, 12524–12528. [CrossRef]
6. Yashima, E.; Maeda, K.; Okamoto, Y. Memory of macromolecular helicity assisted by interaction with achiral small molecules. *Nature* **1999**, *399*, 449–451. [CrossRef]
7. Lee, D.; Jin, Y.J.; Kim, H.; Suzuki, N.; Fujiki, M.; Sakaguchi, T.; Kim, S.K.; Lee, W.E.; Kwak, G. Solvent-to-polymer chirality transfer in intramolecular stack structure. *Macromolecules* **2012**, *45*, 5379–5386. [CrossRef]
8. Jiang, H.J.; Jiang, Y.Q.; Han, J.L.; Zhang, L.; Liu, M.H. Helical nanostructures: Chirality transfer and a photodriven transformation from superhelix to nanokebab. *Angew. Chem. Int. Ed.* **2019**, *58*, 785–790. [CrossRef]
9. Sun, J.; Li, Y.; Yan, F.; Liu, C.; Sang, Y.; Tian, F.; Feng, Q.; Duan, P.; Zhang, L.; Shi, X.; et al. Control over the emerging chirality in supramolecular gels and solutions by chiral microvortices in milliseconds. *Nat. Commun.* **2018**, *9*, 2599. [CrossRef]
10. Cheng, X.X.; Miao, T.F.; Yin, L.; Zhang, W.; Zhu, X.L. Construction of supramolecular chirality in polymer systems: Chiral induction, transfer and application. *Chin. J. Polym. Sci.* **2021**, *39*, 1357–1375. [CrossRef]
11. Huang, S.; Yu, H.; Li, Q. Supramolecular chirality transfer toward chiral aggregation: Asymmetric hierarchical self-assembly. *Adv. Sci.* **2021**, *8*, 2002132. [CrossRef] [PubMed]
12. Nakano, Y.; Ichiyanagi, F.; Naito, M.; Yang, Y.G.; Fujiki, M. Chiroptical generation and inversion during the mirror-symmetry-breaking aggregation of dialkylpolysilanes due to limonene chirality. *Chem. Commun.* **2012**, *48*, 6636–6638. [CrossRef] [PubMed]
13. Zhao, Y.; Rahirn, N.A.A.; Xia, Y.J.; Fujiki, M.; Song, B.; Zhang, Z.B.; Zhang, W.; Zhu, X.L. Supramolecular chirality in achiral polyfluorene: Chiral gelation, memory of chirality, and chiral sensing property. *Macromolecules* **2016**, *49*, 3214–3221. [CrossRef]
14. Zhang, W.; Yoshida, K.; Fujiki, M.; Zhu, X.L. Unpolarized-light-driven amplified chiroptical modulation between chiral aggregation and achiral disaggregation of an azobenzene-alt-fluorene copolymer in limonene. *Macromolecules* **2011**, *44*, 5105–5111. [CrossRef]
15. Wang, L.; Yin, L.; Zhang, W.; Zhu, X.; Fujiki, M. Circularly polarized light with sense and wavelengths to regulate azobenzene supramolecular chirality in optofluidic medium. *J. Am. Chem. Soc.* **2017**, *139*, 13218–13226. [CrossRef] [PubMed]
16. Tejedor, R.M.; Oriol, L.; Serrano, J.L.; Urena, F.P.; Gonzalez, J.J.L. Photoinduced chiral nematic organization in an achiral glassy nematic azopolymer. *Adv. Funct. Mater.* **2007**, *17*, 3486–3492. [CrossRef]
17. Tejedor, R.M.; Millaruelo, M.; Oriol, L.; Serrano, J.L.; Alcala, R.; Rodriguez, F.J.; Villacampa, B. Photoinduced supramolecular chirality in side-chain liquid crystalline azopolymers. *J. Mater. Chem.* **2006**, *16*, 1674–1680. [CrossRef]
18. Akagi, K. Helical polyacetylene: Asymmetric polymerization in a chiral liquid-crystal field. *Chem. Rev.* **2009**, *109*, 5354–5401. [CrossRef]
19. Yamakawa, S.; Wada, K.; Hidaka, M.; Hanasaki, T.; Akagi, K. Chiral liquid-crystalline ionic liquid systems useful for electrochemical polymerization that affords helical conjugated polymers. *Adv. Funct. Mater.* **2019**, *29*, 1806592. [CrossRef]
20. Abdul Rahim, N.A.; Fujiki, M. Aggregation-induced scaffolding: Photoscissable helical polysilane generates circularly polarized luminescent polyfluorene. *Polym. Chem.* **2016**, *7*, 4618–4629. [CrossRef]
21. Hanif, Z.; Choi, D.; Tariq, M.Z.; La, M.; Park, S.J. Water-stable flexible nanocellulose chiral nematic films through acid vapor cross-linked glutaraldehyde for chiral nematic templating. *ACS Macro Lett.* **2020**, *9*, 146–151. [CrossRef]
22. Li, M.-C.; Ousaka, N.; Wang, H.-F.; Yashima, E.; Ho, R.-M. Chirality control and its memory at microphase-separated interface of self-assembled chiral block copolymers for nanostructured chiral materials. *ACS Macro Lett.* **2017**, *6*, 980–986. [CrossRef]
23. Jiang, S.Q.; Zhao, Y.; Wang, L.; Yin, L.B.; Zhang, Z.B.; Zhu, J.; Zhang, W.; Zhu, X.L. Photocontrollable induction of supramolecular chirality in achiral side chain azo-containing polymers through preferential chiral solvation. *Polym. Chem.* **2015**, *6*, 4230–4239. [CrossRef]
24. Gopal, A.; Hifsudheen, M.; Furumi, S.; Takeuchi, M.; Ajayaghosh, A. Thermally assisted photonic inversion of supramolecular handedness. *Angew. Chem. Int. Ed.* **2012**, *51*, 10505–10509. [CrossRef] [PubMed]
25. Stepanenko, V.; Li, X.Q.; Gershberg, J.; Wurthner, F. Evidence for kinetic nucleation in helical nanofiber formation directed by chiral solvent for a perylene bisimide organogelator. *Chem. A Eur. J.* **2013**, *19*, 4176–4183. [CrossRef]
26. Ishikawa, M.; Taura, D.; Maeda, K.; Yashima, E. An optically active hydrogel composed of cross-linked poly(4-carboxyphenyl isocyanide) with a macromolecular helicity memory. *Chem. Lett.* **2004**, *33*, 550–551. [CrossRef]
27. Wang, Y.; Li, Q. Light-driven chiral molecular switches or motors in liquid crystals. *Adv. Mater.* **2012**, *24*, 1926–1945. [CrossRef] [PubMed]
28. Bisoyi, H.K.; Li, Q. Light-directed dynamic chirality inversion in functional self-organized helical superstructures. *Angew. Chem. Int. Ed.* **2016**, *55*, 2994–3010. [CrossRef]

29. San Jose, B.A.; Yan, J.; Akagi, K. Dynamic switching of the circularly polarized luminescence of disubstituted polyacetylene by selective transmission through a thermotropic chiral nematic liquid crystal. *Angew. Chem. Int. Ed.* **2014**, *53*, 10641–10644. [CrossRef]

30. Farooq, M.A.; Wei, W.; Xiong, H. Chiral photonic liquid crystalline polyethers with widely tunable helical superstructures. *Langmuir* **2020**, *36*, 3072–3079. [CrossRef]

31. Jiang, Y.; Cong, Y.; Zhang, B. Synthesis and characterization of chiral smectic side-chain liquid crystalline elastomers containing nematic and chiral mesogens. *New J. Chem.* **2016**, *40*, 9352–9360. [CrossRef]

32. Cheng, X.; Miao, T.; Ma, Y.; Zhu, X.; Zhang, W.; Zhu, X. Controlling multiple chiroptical inversion in biphasic liquid-crystalline polymers. *Angew. Chem. Int. Ed.* **2021**, *60*, 24430–24436. [CrossRef] [PubMed]

33. Saccone, M.; Pfletscher, M.; Dautzenberg, E.; Dong, R.Y.; Michal, C.A.; Giese, M. Hydrogen-bonded liquid crystals with broad-range blue phases. *J. Mater. Chem. C.* **2019**, *7*, 3150–3153. [CrossRef]

34. Wang, H.; Bisoyi, H.K.; Li, B.X.; McConney, M.E.; Bunning, T.J.; Li, Q. Visible-light-driven halogen bond donor based molecular switches: From reversible unwinding to handedness inversion in self-organized soft helical superstructures. *Angew. Chem. Int. Ed.* **2020**, *59*, 2684–2687. [CrossRef]

35. Wang, L.; Urbas, A.M.; Li, Q. Nature-inspired emerging chiral liquid crystal nanostructures: From molecular self-assembly to DNA mesophase and nanocolloids. *Adv. Mater.* **2020**, *32*, 1801335. [CrossRef]

36. Zheng, Z.G.; Lu, Y.Q.; Li, Q. Photoprogrammable mesogenic soft helical architectures: A promising avenue toward future chiro-optics. *Adv. Mater.* **2020**, *32*, 1905318. [CrossRef]

37. Zhao, Y.; Zhang, L.; He, Z.; Chen, G.; Wang, D.; Zhang, H.; Yang, H. Photoinduced polymer-stabilised chiral nematic liquid crystal films reflecting both right- and left-circularly polarised light. *Liq. Cryst.* **2015**, *42*, 1120–1123. [CrossRef]

38. Kulkarni, C.; Curvers, R.H.N.; Vantomme, C.; Broer, D.J.; Palmans, A.R.A.; Meskers, S.C.J.; Meijer, E.W. Consequences of chirality in directing the pathway of cholesteric helix inversion of pi-conjugated polymers by light. *Adv. Mater.* **2021**, *33*, 2005720. [CrossRef]

39. Wu, Y.L.; Natansohn, A.; Rochon, P. Photoinduced chirality in thin films of achiral polymer liquid crystals containing azobenzene chromophores. *Macromolecules* **2004**, *37*, 6801–6805. [CrossRef]

40. Miao, T.F.; Cheng, X.X.; Ma, H.T.; He, Z.X.; Zhang, Z.B.; Zhou, N.A.C.; Zhang, W.; Zhu, X.L. Transfer, amplification, storage, and complete self-recovery of supramolecular chirality in an achiral polymer system. *Angew. Chem. Int. Ed.* **2021**, *60*, 18566–18571. [CrossRef] [PubMed]

41. Kani, R.; Nakano, Y.; Hayase, S. Photochemical and thermal-properties of polysilane lb films—stabilization of oriented polysilane lb films by cross-linking. *Macromolecules* **1995**, *28*, 1773–1777. [CrossRef]

42. Cheng, Z.X.; Ma, S.D.; Zhang, Y.H.; Huang, S.; Chen, Y.X.; Yu, H.F. Photomechanical motion of liquid-crystalline fibers bending away from a light source. *Macromolecules* **2017**, *50*, 8317–8324. [CrossRef]

43. Xia, Q.; Meng, L.; He, T.; Huang, G.; Li, B.S.; Tang, B.Z. Direct visualization of chiral amplification of chiral aggregation induced emission molecules in nematic liquid crystals. *ACS Nano* **2021**, *15*, 4956–4966. [CrossRef] [PubMed]

44. Berova, N.; Di Bari, L.; Pescitelli, G. Application of electronic circular dichroism in configurational and conformational analysis of organic compounds. *Chem. Soc. Rev.* **2007**, *36*, 914–931. [CrossRef]

45. Ikeda, T.; Tsutsumi, O. Optical switching and image storage by means of azobenzene liquid-crystal films. *Science* **1995**, *268*, 1873–1875. [CrossRef] [PubMed]

46. Yin, L.; Zhao, Y.; Jiang, S.Q.; Wang, L.B.; Zhang, Z.B.; Zhu, J.; Zhang, W.; Zhu, X.L. Preferential chiral solvation induced supramolecular chirality in optically inactive star azo polymers: Photocontrollability, chiral amplification and topological effects. *Polym. Chem.* **2015**, *6*, 7045–7052. [CrossRef]

47. Miao, T.F.; Yin, L.; Cheng, X.X.; Zhao, Y.; Hou, W.J.; Zhang, W.; Zhu, X.L. Chirality construction from preferred pi-pi stacks of achiral azobenzene units in polymer: Chiral induction, transfer and memory. *Polymers* **2018**, *10*, 612. [CrossRef]